# Quantitative Evaluation of Iodine-123 Hippuran Gamma Camera Renography in Normal Children

Ove Carlsen, Birgit Kvinesdal, and Erling Nathan

*Isotope Laboratory, Vejle Hospital, Vejle, Denmark; and Pediatric Department, Kolding Hospital, Kolding, Denmark*

In a retrospective study of 39 normal children submitted to [$^{123}$I]hippuran gamma camera renography, a quantitative evaluation of the recorded data showed that: (a) the rate constant for renal plasma clearance of [$^{123}$I]hippuran was $-0.166 \pm 0.043$ min$^{-1}$ corresponding to a hippuran plasma clearance of $518 \pm 142$ ml/min per 1.73 m$^2$; (b) the fractional renal clearance of [$^{123}$I]hippuran was $0.51 \pm 0.03$ and $0.49 \pm 0.03$ for the left and the right kidney, respectively; and (c) the mean values for the mean transit times of [$^{123}$I]hippuran through the whole kidney,the renal parenchyma, and the renal pelvis, respectively, were 4.2, 1.9, and 2.5 min. Five kidneys (in four patients) showed prolonged renal mean transit times of [$^{123}$I]hippuran. Follow-up renographies were performed in three of the four children and gave normal results. Patients with renal mean transit times above the present 5% significance limit of 8.2 min should not necessarily be considered having an abnormal renal function.

J Nucl Med 27:117–127, 1986

Since 1956 when Taplin and co-workers first introduced the radioisotope renogram, the publications concerning this subject by now probably number well over a thousand. The interpretation of the renographic data was performed in a purely qualitative manner by visual inspection of the recorded curves.

Later, the visual assessment was replaced by semiquantitative methods based on values of certain empirical parameters obtained from simple measurements on the renograms (heights, slopes, peak times, residual renal activities, etc.).

The introduction of the gamma camera and the computer in nuclear medicine has resulted in many attempts at quantitative analysis of radioisotope renography (*1*,*2*).

The determination of the renal indicator clearance in renography usually comprises a computer-assisted analysis of the activity-time curve for a region of interest in the body and one or more blood samples drawn at different times during the renography (*3–6*). In this work, the evaluation of the renal indicator clearance is expressed as the ratio of the indicator clearance to its vascular distribution volume. Blood samples are not required. The presentation should be regarded as an alternative way of adjustment of the renal indicator clearance, and it is perhaps as correct as the usual one of adjusting to a standard body surface of 1.73 m$^2$.

The complete description of the passage of an indicator through a kidney is given by the residual impulse response for that kidney (with respect to the indicator). We have derived a direct computational algorithm based on Laplace transforms for determination of the residual impulse response. This algorithm is likely to be less sensitive to noise on the renographic data as compared with the matrix algorithm of deconvolution used by others (*7*).

The residual impulse responses for the whole kidney and for the renal parenchyma alone are determined in this work. Knowledge of these residual impulse responses makes it possible to distinguish between obstructive uropathy and obstructive nephropathy (*8*,*9*).

If the residual impulse response should be described by a single parameter, this parameter would be the mean transit time. Consequently, the mean transit times of indicator through the kidney and the renal parenchyma are the most clinically useful single parameters for assessment of whether an outflow obstruction from a kidney will induce loss of nephrons.

Received Nov. 26, 1984; revision accepted Aug. 9, 1985.

For reprints contact: Ove Carlsen, MSc, Isotope Laboratory, Vejle Hospital, DK-7100 Vejle, Denmark.

**TABLE 1**
**Classification of Patient Material After [$^{123}$I]Hippuran Gamma Camera Renography**

| | | |
|---|---|---|
| Patients with normal findings prior to the IHGR | | 39 |
| Patients with abnormal findings prior to the IHGR | | 49 |
| (a) Vesico-ureteral reflux | 23 | |
| (b) Obstructive uropathy | 10 | |
| (c) Pyelonephritis | 6 | |
| (d) Renal aplasia/dysplasia | 5 | |
| (e) Glomerulonephritis | 2 | |
| (f) Neurogenic bladder | 2 | |
| (g) Nephrectomy | 1 | |
| Patients who had not been submitted to all examinations | | 11 |
| Patients in whom the IHGR failed | | 10 |
| (a) Patient movements | 2 | |
| (b) Unsuccessful i.v. injection | 4 | |
| (c) Technical errors | 4 | |
| | Total 109 | |

## MATERIALS AND METHODS

### Normal Subject Selection

During the period December 1981-March 1983, a total of 109 patients 2-15 yr old were referred to the pediatric department of our institution with renal and urological disorders, predominantly urinary tract infections (UTI).

Intravenous pyelography, microscopy of the urine, quantitative bacterial count, stix for protein and glucose in the urine, and se-carbamid were performed in all patients. UTI was treated with antibiotics for 10 days followed by prophylactic nitrofurantoin treatment (1-2 mg/kg/day). After a minimum of 4 mo without UTI, micturating cysto-urethrography (MCU) and iodine-123 ($^{123}$I) hippuran gamma camera renography (IHGR) were made.

Classification of the patients at the time of the IHGR is shown in Table 1. Of the 109 children, 39 (two boys, 37 girls) could be considered normal. The mean age was 7.9 yr.

In all children (except five), the IHGR was performed on the day after the MCU. Approximately half an hour prior to the IHGR, the children were asked to drink juice to stimulate the diuresis. The radioactive dose for the children was calculated as follows: (4 × age + 20)/100 mCi [$^{123}$I]hippuran.

### Renographic Imaging Protocol

A gamma camera with a 40-cm field-of-view and mounted with a low-energy, high-resolution parallel hole collimator was used. Patients were lying in the supine position with the detector head opposite to the kidney region from the dorsal side. Following a bolus injection into the median cubital vein of the radioactive indicator, digital images were recorded for 30-40 min postinjection using three sampling rates: 0-5 min: 5 sec/frame, 5-20 min: 20 sec/frame, and 20-40 min: 1 min/frame. Frames were collected in a 64 × 64 matrix. The energy window setting around the photon peak was 20%.

### Image Analysis

In the digital images, regions of interest (ROIs) were visually placed over: (a) the heart, mainly over the left ventricle; (b) the right liver lobe well outside the contour of the right kidney; (c) the left kidney; (d) the parenchyma of the left kidney; (e) the right kidney; and (f) the parenchyma of the right kidney. The parenchymal curves are based on the activity within a 2-3-cells-wide ROI running from the upper to the lower pole along the lateral contour of the kidney. Hence, the parenchymal curves represent the activities in nephrons distributed predominantly in the renal cortex. The kidney curves (i.e., the renograms) include the whole of the renal pelvis. The above six activity-time curves constitute the basic data material in the subsequent analysis in the computer.

### Analysis and Decomposition of the Heart Curve

The heart curve is assumed to measure only the radiation from indicator distributed in the vascular pool within the cardiac ROI. This plasma volume is denoted $V_{hp}$. Let $t = t_o$ denote the time after injection when the bolus has mixed with the plasma. We use as $t_o$ the peak time of the heart curve plus 45 sec, i.e., $t_o$ is ~1 min after injection. The plasma concentration of indicator in the volume $V_{hp}$ is denoted $C_{hp}(t)$ and $C_p(t)$ in the total plasma volume, $V_p$ (for $t \geq t_o$). We get for the heart curve H(t):

$$H(t) = G_h V_{hp} C_{hp}(t) = G_h V_{hp} C_p(t) \quad (\text{for } t \geq t_o). \tag{1}$$

The factor $G_h$ in Eq. (1) takes into account the measurement geometry of the indicator within the volume $V_{hp}$. Further, $G_h$ includes the sensitivity of the gamma camera and subsequent electronic equipment. The dimension of $G_h$ is, for example, count rate per $\mu$Ci of the radioisotope. H(t) represents a count rate.

Let $F_{pk}$ denote the renal plasma clearance of the indicator. The rate constant for renal clearance of the indicator is defined as follows:

$$\lambda_{pk} = -F_{pk}/V_p. \tag{2}$$

For the computation of the rate constant $\lambda_{pk}$, we will use the Stewart-Hamilton method from the theory of stochastic tracer analysis. This method states that the (effective) carrier flow through a system is given by the ratio of the injected dose to the integral from t = o to infinity of the tracer concentration at the output side of the system.

The method can be expressed as:

$$F_{pk} = \frac{Q}{\int_o^\infty C_{hp}(t)dt}, \tag{3}$$

where Q denotes the dose injected (in $\mu$Ci). We assume that the plasma concentrations of indicator at the output side of the system, i.e., in the renal arteries, is identical to $C_{hp}(t)$.

Combination of Eqs. (1)-(3) gives after rearrangement:

$$\lambda_{pk} = -\frac{G_h(V_{hp}/V_p)Q}{\int_o^\infty H(t)dt}. \tag{4}$$

Let $Q_p(t_o)$ and $Q_e(t_o)$ denote, respectively, the parts of the dose Q which at time $t_o$ reside in the plasma volume $V_p$ and in the extravascular distribution volume $V_e$. The measurement of hippuran clearance starts at time $t_o$ instead of at zero time.

Equation (4) is then rearranged as follows:

$$\lambda_{pk} = -\frac{G_h(V_{hp}/V_p)(Q_p(t_o) + Q_e(t_o))}{\int_{t_o}^{\infty} H(t)dt}. \quad (5)$$

In the time interval from $t = t_o$ to the end of the renography, the heart curve is approximated by a biexponential expression:

$$H(t) = H_1 e^{\lambda_1(t - t_o)} + H_2 e^{\lambda_2(t - t_o)}. \quad (6)$$

Equation 6 is used for extrapolation of H(t) to infinity. The biexponential decomposition of the heart curve is based on Marquardt's iterative least-squares method (*1,10*). The biexponential expression for H(t) is consistent with a prerenal kinetic model for the indicator consisting of an open two compartmental model. This is shown in Appendix 1.

The quantity $G_h(V_{hp}/V_p)Q_p(t_o)$ can be interpreted as the count rate within the cardiac ROI when $Q_p(t_o)$ is uniformly distributed in $V_p$. Hence, $G_h(V_{hp}/V_p)Q_p(t_o)$ must equal $H(t_o)$. We then have:

$$\lambda_{pk} = \frac{(H_1 + H_2)(1 + R_q)}{H_1/\lambda_1 + H_2/\lambda_2}, \quad (7)$$

where $R_q$ denotes the ratio $Q_e(t_o)/Q_p(t_o)$.

Owing to the considerable extravascular clearance of hippuran during the first circulation of the injection bolus, we assume that at time $t_o$ a state of approximate concentration equilibrium exists between the plasma volume $V_p$ and the extravascular hippuran distribution volume $V_e$. Becker (*11*) found for [$^{131}$I]hippuran a concentration equilibrium between $V_p$ and $V_e$ 5 min postinjection as an average value in eight patients. Hence, the ratio $R_q$ must equal the ratio $V_e/V_p$ as an approximation.

The ratio $V_e/V_p$ remains to be evaluated. The slow component of the heart curve, $H_2e^{\lambda_2(t-t_o)}$, is considered proportional to the concentration curve for [$^{123}$I]hippuran in the plasma if $Q_p(t_o)$ was distributed at time $t_o$ uniformly in $V_p$ and in $V_e$.

We have:

$$H_1 + H_2 = G_h V_{hp} Q_p(t_o)/V_p \quad (8)$$

and

$$H_2 = G_h V_{hp} Q_p(t_o)/(V_p + V_e). \quad (9)$$

Solution of Eqs. (8)-(9) for $V_e/V_p$ yields:

$$V_e/V_p = H_1/H_2. \quad (10)$$

The final expression for calculation of the rate constant for clearance of [$^{123}$I]hippuran reads:

$$\lambda_{pk} = \frac{(H_1 + H_2)(1 + H_1/H_2)}{H_1/\lambda_1 + H_2/\lambda_2}. \quad (11)$$

### Correction of Kidney Curves for Background Radiation

The correction of the left and right kidney curves for background radiation is made with the following expression:

$$K(t) = CK(t) - SF \cdot RBG(t), \quad (12)$$

where K(t) denotes the kidney curve, CK(t) is the composite kidney curve (i.e., including the background radiation), SF is the subtraction factor, and RBG(t) denotes a reference background curve. The reference background curve is assumed to have a shape identical to the true left and right renal background curves. As RBG(t) we use a smoothed version of the activity curve for a ROI recorded over the right liver lobe well outside the contour of the right kidney.

The subtraction factor of a kidney curve is calculated from CK(t), RBG(t), and the heart curve, H(t), using the following expression:

$$SF = \frac{CK(t_o) - R \cdot \Delta CK}{RBG(t_o) - R \cdot \Delta RBG}, \quad (13)$$

where

$$\Delta CK = CK(t_o + \Delta t) - CK(t_o),$$

$$\Delta RBG = RBG(t_o + \Delta t) - RBG(t_o) \text{ and}$$

$$R = \int_0^{t_o} H(t)dt \Big/ \int_{t_o}^{t_o + \Delta t} H(t)dt.$$

The time $t = t_o + \Delta t$ chosen excludes that any indicator has left the kidney before this time. Usually, $t_o + \Delta t$ is ~2 min postinjection. For details of the calculation of the subtraction factor SF see Appendix 2.

Compared with the renograms, the correction of the composite parenchymal curves for background radiation is more simple. The subtraction factor for a parenchymal curve is equal to the product of the subtraction factor for the corresponding kidney curve and the fraction of the size of the parenchymal ROI to that of the renal ROI. The parenchymal curves are multiplied by a factor so that they fit their respective kidney curves until the time when the indicator begins to leave the renal parenchyma on that side. In this way, a correct parenchymal curve should run below the kidney curve during the time of removal of indicator from the kidney to demonstrate a delay of indicator in the calyces and/or pelvis.

### Computation of the Kidney Residual Impulse Response

The kidney impulse response, IR(t), is defined by the convolution integral:

$$\int_0^t IR(T) \cdot KI(t-T)dT = KO(t), \quad (14)$$

where KI(t) and KO(t) denote the kidney input and kidney output, respectively. The dimensions of KI(t) and KO(t) are, for example, count rate/min. The dimension of IR(t) is 1/min. The kidney impulse response is a frequency distribution function, i.e., it tells the proportion of an indicator taken up by the kidney that traverses it in a given time.

The convolution integral in Eq. (14) can be expressed in another form (*1*):

$$\int_0^t RIR(T) \cdot KI(t-T)dT = K(t), \quad (15)$$

where the kidney residual impulse response, RIR(t), is given by:

$$RIR(t) = 1 - \int_0^t IR(T)dT. \quad (16)$$

This way of expressing the convolution integral is more convenient since the kidney curve K(t) is readily available in contrast to the kidney output KO(t).

The kidney input, KI(t), is the derivative with time of the kidney uptake KU(t):

$$KI(t) = \frac{dKU}{dt} \cdot \qquad (17)$$

The kidney uptake KU(t) is defined as the net quantity of indicator that has entered the kidney from the time of injection to an arbitrary time t. The dimension of KU(t) is count rate. When no indicator has left the kidney, the kidney curve and the kidney uptake curve are identical.

Since the kidney input curve is proportional to the heart curve, the kidney uptake can be determined from a curve fit of the kidney curve to the integral of the heart curve in the time interval $t_o \leq t \leq t_d$ where $t = t_d$ is the time when indicator begins to leave the kidney:

$$K(t) = K(t_o) + \sigma \int_{t_o}^{t} H(T)dT. \qquad (18)$$

The results of the linear regression problem in Eq. (18) are $K(t_o)$ and $\sigma$; $K(t_o)$ is the kidney bolus, i.e., the part of the injection bolus Q taken up by the kidney and, of course, $K(t_o)$ represents a count rate in the kidney measurement geometry.

The kidney uptake, KU(t) is given by the expression on the right side of Eq. (18) but valid for all $t \geq t_o$.

The kidney input is determined as the derivative with time of the kidney uptake in Eq. (18):

$$\begin{aligned} KI(t) &= K(t_o) \cdot \delta(t-t_o) + \sigma \cdot H(t) \\ &= K(t_o) \cdot \delta(t-t_o) + \sigma H_1 e^{\lambda_1(t-t_o)} + \sigma H_2 e^{\lambda_2(t-t_o)}. \end{aligned} \qquad (19)$$

In Eq. (19), $\delta(t-t_o)$ represents Dirac's delta-function (i.e., a function with infinite pulse height and infinite small pulse width around $t = t_o$; area of delta-function is 1). The kidney input consists of the sum of an impulse function and a biexponential expresssion.

In the convolution integral in Eq. (15), the kidney input, KI(t), and the kidney curve, K(t), are now both known. The solution of the convolution integral is made using the theory of Laplace transforms.

The formula for the residual impulse response, RIR(t), reads for $t \geq t_o$:

$$RIR(t) = \frac{1}{K(t_o)} \int_{t_o}^{t} \frac{dK}{dt} \cdot \varphi(t-T)dT, \qquad (20)$$

where the function $\varphi(t)$ is a biexponential expression determined by the parameters in the kidney input expression in Eq. (19).

In the calculation of RIR(t) from Eq. (20), the integral is approximated by sums over appropriate small time steps. The derivative of the kidney curve, dK/dt, is approximated by a finite difference quotient after a smoothing of the kidney curve by repeated use of a five-point smoothing algorithm.

The derivation of the analytical solution of the convolution integral with regard to RIR(t) in Eq. (20) is rather cumbersome. It is shown in Appendix 3.

The derivation of the residual impulse response for a parenchymal curve and for a kidney curve is the same.

## Mean Transit Times of Indicator Through the Renal Parenchyma and the Renal Pelvis

The mean transit time, MTT, of an indicator through a system is determined by the expression:

$$MTT = \int_{o}^{\infty} t \cdot IR(t)dt, \qquad (21)$$

where IR(t) denotes the impulse response of the system with regard to the indicator.

By introducing the residual impulse response of the system defined in Eq. (16), the formula for MTT in Eq. (21) can be rearranged using partial integration to yield:

$$MTT = \int_{o}^{\infty} RIR(t)dt. \qquad (22)$$

Hence, the mean transit time is the area under the residual impulse response curve from zero time to infinity.

Since the residual impulse responses for the kidney and the renal parenchyma have been determined in the preceding paragraph, the mean transit time through the kidney, $MTT_k$, and that through the renal parenchyma, $MTT_a$, can easily be calculated. Mean transit times of subsystems in series are additive. Thus, the mean transit time through the renal pelvis, $MTT_e$, is given by:

$$MTT_e = MTT_k - MTT_a.$$

Figure 1 shows an example of the residual impulse response curves of [$^{123}$I]hippuran for a kidney and its parenchyma.

### Fractional Renal Clearances

The fractional contributions to the total renal indicator clearance by the left and right kidneys are denoted $FRC_l$ and $FRC_r$, respectively; $FRC_l + FRC_r = 1$.

Let $\sigma_l$ and $\sigma_r$ denote the values of $\sigma$ in the curve fit in Eq. (18) for the left and right kidney, respectively. Then we have:

$$FRC_l = \sigma_l/(\sigma_l + \sigma_r) \text{ and}$$
$$FRC_r = \sigma_r/(\sigma_l + \sigma_r).$$

The rate constants for indicator clearance by the left and

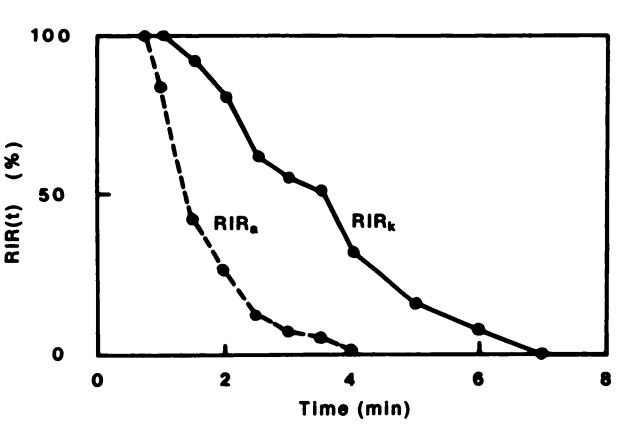


**FIGURE 1**
**Residual impulse response of [$^{123}$I]hippuran for left kidney ($RIR_k$) and parenchyma of left kidney ($RIR_a$) in 13-yr-old normal girl. Mean transit time through kidney, $MTT_k$, is 3.4 min and that for renal parenchyma, $MTT_a$, 1.7 min. Zero time is ~1 min after injection**

**TABLE 2**
Mean Values and Standard Deviations of Rate Constants for Renal Clearance and Fractional Renal Clearance of [$^{123}$I]Hippuran for Left and Right Kidney in 39 Normal Children

| Item | Mean | Standard deviation | 5% Significance limits | |
|---|---|---|---|---|
| Both kidneys, $\lambda_{pk}$ ($min^{-1}$) | −0.166 | 0.043 | −0.081 | −0.25 |
| Left kidney, $\lambda_{pk,l}$ ($min^{-1}$) | −0.084 | 0.023 | −0.038 | −0.13 |
| Right kidney, $\lambda_{pk,r}$ ($min^{-1}$) | −0.078 | 0.021 | −0.038 | −0.12 |
| Left kidney, $FRC_l$ | 0.507 | 0.031 | 0.45 | 0.57 |
| Right kidney, $FRC_r$ | 0.493 | 0.031 | 0.43 | 0.55 |

right kidney, $\lambda_{pk,l}$ and $\lambda_{pk,r}$, respectively, are calculated as:

$$\lambda_{pk,l} = FRC_l \cdot \lambda_{pk} \text{ and}$$

$$\lambda_{pk,r} = FRC_r \cdot \lambda_{pk}.$$

The biexponential decomposition of the heart curve [Eq. (6)] includes a statistical evaluation of the parameters determined, i.e., the standard deviations (s.d.s) and correlation coefficients for $H_1$, $\lambda_1$, $H_2$, and $\lambda_2$ (*1*). The linear regression problem in Eq. (18) also includes a statistical investigation. The total statistical information makes it possible to evaluate the s.d.s of $\lambda_{pk}$, $\lambda_{pk,l}$, $\lambda_{pk,r}$ and of $FRC_l$ and $FRC_r$. Stochastic simulation is used for this purpose.

### Accuracy of the Quantitative Method

The accuracy of the rate constant for renal clearance of [$^{123}$I]hippuran has been investigated by comparison of $\lambda_{pk}$ with the standard glomerular filtration rate in a study of 31 patients (15 men, 16 women) submitted to IHGR at our institution, during the period December 1981–May 1985. The age distribution was 45 ± 19 yr. The glomerular filtration rate was determined by chromium-51 ethylenediaminetetraacetic acid clearance in 27 patients and by creatinine clearance with urine sampling in four patients. The maximum time interval between the IHGR and the clearance determination was chosen as 2 mo. For the patient material, the time interval was 23 ± 19 days. All patients were in a nonacute state of renal disease, most of them having a long history of renal diseases. The values of the glomerular filtration rates were distributed over the interval 10–130 ml/min per 1.73 $m^2$.

### Precision of the Quantitative Method

The precision of the quantitative evaluation of the gamma camera renography has been studied by repeated generation and computation of the ROI curves in a patient study of 40 children and adults with/without renal diseases. The patients were selected from a total of 300 patients submitted to IHGR at the isotope laboratory, Vejle Hospital, during the period December 1981–April 1984. Both the original and the new generation of ROI curves were made by the same experienced computer operator.

## RESULTS

### Rate Constants for Renal Clearance of [$^{123}$I]Hippuran

The total ($\lambda_{pk}$), the left ($\lambda_{pk,l}$) and the right ($\lambda_{pk,r}$) rate constant for renal plasma clearance of [$^{123}$I]hippuran are presented with means and s.d.s in Table 2. The 5% significance limits are included. Chi-square tests of goodness of fit were made to test the hypothesis that the histograms of the three variables could be described by normal distributions (*12*). All three tests turned out nonsignificant ($p<0.15$, $p<0.25$, and $p<0.30$, respectively). The means of $\lambda_{pk}$, $\lambda_{pk,l}$, and $\lambda_{pk,r}$ in the table are calculated as weighted means where the weights are the inverse variances of the three variables for each patient.

### Accuracy of the Rate Constant for Renal Clearance of [$^{123}$I]Hippuran

Linear regression of $|\lambda_{pk}|$ compared with standard glomerular filtration rate, SGFR, in ml/min in 31 patients yielded:

$$|\lambda_{pk}| = a \cdot SGFR + b,$$

where

$$a = 0.00129 \pm 0.00011 \text{ ml}^{-1} \ (\bar{x} \pm 1 \text{ s.e.m.})$$

and

$$b = 0.0059 \pm 0.0079 \text{ min}^{-1} \ (\bar{x} \pm 1 \text{ s.e.m.}).$$

The s.d. of the data around the regression line was 0.022 $min^{-1}$ while the linear correlation coefficient was 0.90.

### Fractional Renal Clearance of [$^{123}$I]Hippuran

The mean value and s.d. for the fractional renal clearance of [$^{123}$I]hippuran of the left ($FRC_l$) and the right ($FRC_r$) kidney are shown in Table 2. The 5% significance limits are included.

A Chi-square test of goodness-of-fit was made to test the hypothesis that the histogram of the variable $FRC_l$ could be described by a normal distribution (*12*). The test was nonsignificant ($p<0.41$). The means of $FRC_l$ and $FRC_r$ in the table are calculated as weighted means where the weights are the inverse variances of the two variables for each patient.

### Mean Transit Times of Indicator

The mean transit times (MTT) of [$^{123}$I]hippuran through the kidney, the renal parenchyma, and the renal pelvis are shown as histograms in Fig. 2 for the whole patient material of 39 children. No distinction between the left and right kidneys has been made.

Logarithmic normal curves were fitted to the histograms in Fig. 2. Chi-square tests of goodness-of-fit were made to test the hypothesis that the histograms could be described by

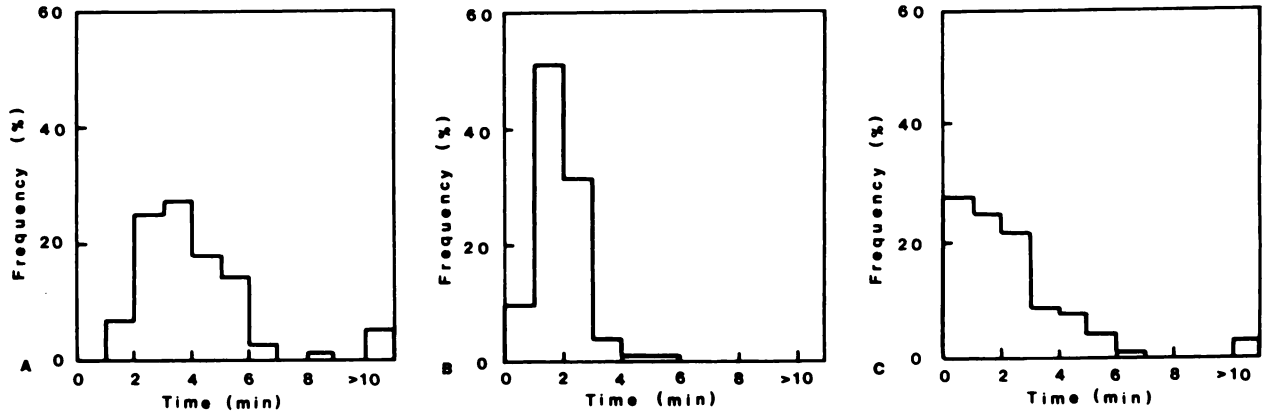


**FIGURE 2**
Histograms of MTTs of [$^{123}$I]hippuran through kidneys (A), renal parenchyma (B), and renal pelvis (C) in 39 normal children

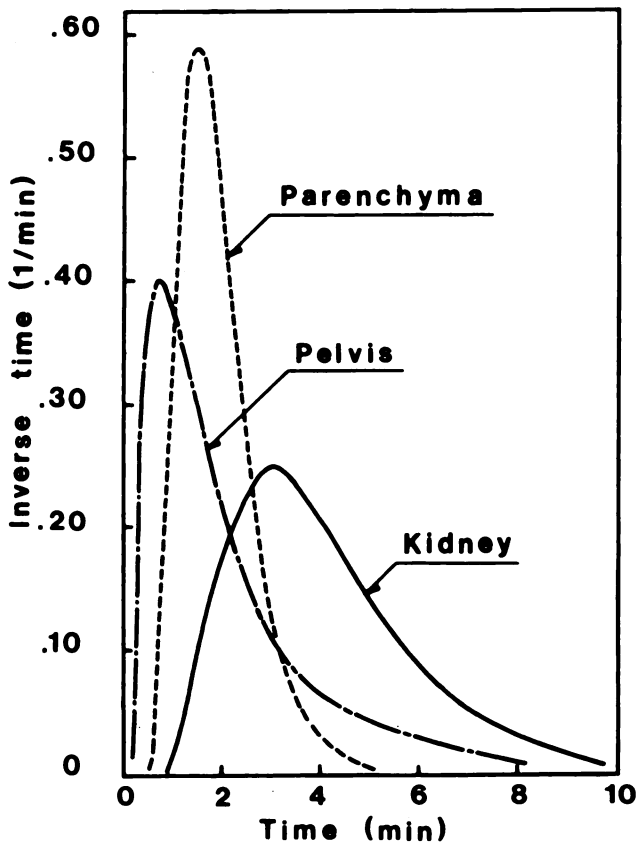


**FIGURE 3**
Logarithmic normal curve fits to histograms of MTT of [$^{123}$I]hippuran through kidneys, renal parenchyma, and renal pelvis in 39 normal children

logarithmic normal curves (*12*). All three tests were nonsignificant ($p<0.29$, $p<0.22$, and $p<0.37$, respectively). The three logarithmic normal curves are shown together in Fig. 3 for comparison. It is seen that the skewness of the distribution of mean transit times is considerably greater for the renal pelvis than for the renal parenchyma. The latter is nearly symmetrically distributed around 1.7 min, whereas the distribution of the mean pelvis transit times have a mode value below 1 min, but a mean value of 2.5 min. The mode, median, and mean values of the logarithmic normal curves are given in Table 3 together with the 5% one-tailed upper significance limits.

Five kidneys (in four patients) had prolonged renal MTT-values ($p<0.05$), mainly owing to prolonged parenchymal or pelvic MTT-values. The shapes of the five renograms differed considerably from those of the remaining 73 kidneys. The renograms of the four patients are shown in Fig. 4. Gross estimates of the diuresis based on urine collection yielded 7.0, 0.2, 0.7, and 2.5 ml/min/1.73 m$^2$ in Patients I–IV, respectively. However, follow-up IHGR performed in Patients I, II, and IV resulted in normal renal MTT-values. The follow-up IHGR were not included in this study.

### Precision of the Quantitative Method

To test the hypothesis that the variable values in the first and second generation and analysis of data have been drawn from populations with identical mean values, the Wilcoxon matched-pairs signed-ranks test have been applied (*13*). The tests for the first six variables listed in Table 4 were nonsignificant. The test for $MTT_e$ was significant at the 5% significance level. All tests were two-tailed. The mean values of the seven variables in the first and second analysis of the 40 IHGR are presented in Table 4. Included in the table is a quantitative evaluation of the precisions of

**TABLE 3**
Mode, Median, and Mean Values of Logarithmic Normal Curve Fits to Histograms in Fig. 2

| Item | Mode (min) | Median (min) | Mean (min) | Upper 5% significance limit (min) |
|---|---|---|---|---|
| Kidney | 3.0 | 3.8 | 4.2 | 8.2 |
| Renal parenchyma | 1.5 | 1.7 | 1.9 | 3.4 |
| Renal pelvis | 0.72 | 1.7 | 2.5 | 7.4 |

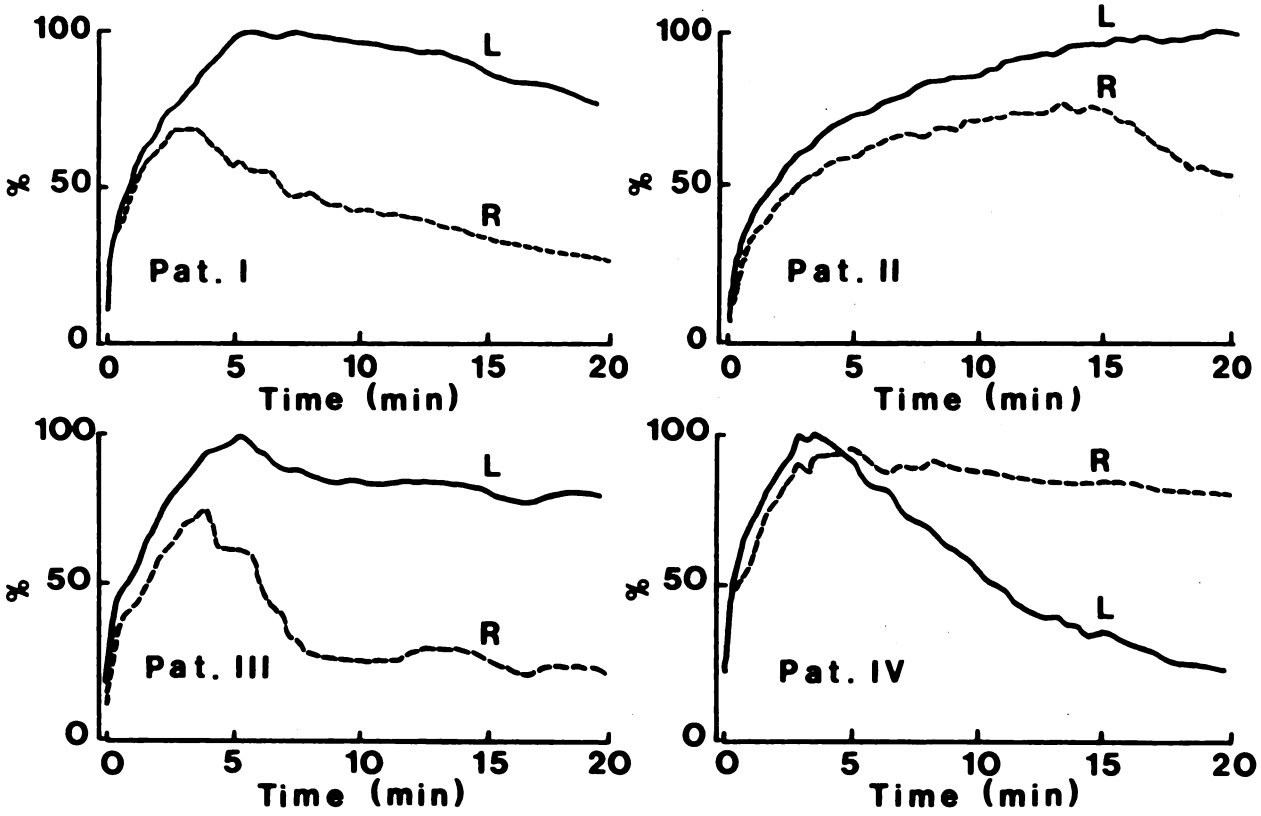


**FIGURE 4**
Recorded left and right renograms in four normal children with prolonged MTTs of [$^{123}$I]hippuran through one or both kidneys

**TABLE 4**
Precision of Variables Derived from Quantitative Analysis of [$^{123}$I]Hippuran Gamma Camera Renography in 40 Patients With/Without Renal Diseases

| Variable | First generation and analysis of data | | Second generation and analysis of data | | Absolute precision | Relative precision for mean value (%) |
|---|---|---|---|---|---|---|
| | Number | Mean | Number | Mean | | |
| $/\lambda_{pk}/$ ($min^{-1}$) | 40 | 0.131 | 40 | 0.128 | 0.0068 | 5.3 |
| $/\lambda_{pk,l}/$ ($min^{-1}$) | 37 | 0.071 | 37 | 0.069 | 0.0040 | 5.7 |
| $/\lambda_{pk,r}/$ ($min^{-1}$) | 40 | 0.065 | 39 | 0.066 | 0.0048 | 7.3 |
| $FRC_l$ | 37 | 0.52 | 37 | 0.52 | 0.017 | 3.3 |
| $MTT_k$ (min) | 77 | 6.3 | 76 | 5.8 | 0.42 | 6.9 |
| $MTT_a$ (min) | 67 | 3.0 | 70 | 3.5 | 0.42 | 12.9 |
| $MTT_e$ (min) | 67 | 2.2 | 70 | 1.9 | 0.25 | 12.5 |

the variables expressed as the standard deviations of the double determinations (*14*).

## DISCUSSION

We are aware that strictly speaking none of the children can be considered normal, since the indication for making the various examinations (including the IHGR) was recurrent urinary tract infections. However, the 39 children had been free from infection for at least 4 mo prior to the IHGR and had normal findings at all other examinations. We therefore believe that our patient material is close to a genuine normal material.

According to Wesson (*15*), the effective renal plasma flow or the PAH-clearance in girls at the age of 8 yr is 590 ± 115 ml/min per 1.73 $m^2$. The total renal plasma flow, TRPF, is 638 ± 124 ml/min per 1.73 $m^2$. This estimation was made by dividing the PAH-clearance by the normal mean extraction ratio of PAH, $E_{PAH}$, of 92.5% (*13*). We have chosen girls as reference since 37 of the 39 children are girls (mean age 8 yr).

After a single injection of [$^{125}$I] or [$^{131}$I]hippuran,

Pihl (*16*) found that the mean renal extraction ratios in nine normal adults were, respectively, 92, 79, 77, and 76% at injection time, 10, 20, and 30 min postinjection. A normal mean [$^{123}$I]hippuran extraction ratio, $E_{HIP}$, during 30 min can be calculated as 80%. The mean duration of the IHGR was 32 min. The [$^{123}$I]hippuran clearance, $F_{pk}$, is equal to $E_{HIP}$ TRPF or 510 ± 100 ml/min per 1.73 m$^2$ for girls at the age of 8 yr.

Pihl (*16*), Magnusson (*17*), and Becker (*11*) investigated the red cell uptake of hippuran. After a single injection of hippuran, they have all shown that ~24% of the hippuran is in the red cells ~30 min postinjection. Hence, a part of the red cell volume must be included in the vascular hippuran distribution volume, denoted $V_d$.

$V_d$ can be calculated as:

$$V_d = V_b \cdot BSA\ (1 - Ht)/(1 - CBQR),$$

where $V_b$ is the blood volume per m$^2$ body surface area, BSA; Ht is the hematocrit and CBQR denotes the Cell-to-Blood Quantity Ratio (CBQR) of hippuran.

$V_b$ is 2,245 ± 191 ml per m$^2$ in women (*13*), and the normal variation of Ht in 8-yr-old girls is 0.389 ± 0.018 (*13*). For CBQR, we use the 24% mentioned above as a (probably overestimated) mean value for CBQR during 30 min. This gives for $V_d$ 3,122 ± 281 ml per 1.73 m$^2$ corresponding to 2,373 ml plasma and 749 ml red cells. Based on these data from the literature, the rate constant for clearance of [$^{123}$I]hippuran, $-F_{pk}/V_d$, can be evaluated as $-0.163 \pm 0.035$ min$^{-1}$ ($\bar{x} \pm 1$ s.d.). This is in accordance with our finding for $\lambda_{pk}$ of $-0.166 \pm 0.043$ min$^{-1}$ ($\bar{x} \pm 1$ s.d.) in the normal pediatric material.

The linear regression of $/\lambda_{pk}/$ compared with SGFR shows that the constant term is not significantly different from zero ($p<0.45$). Hence, direct proportionality between $/\lambda_{pk}/$ and SGFR for SGFR in the range 10–130 ml/min has been established.

The theoretical slope of the regression line is:

$$|\lambda_{pk}|/SGFR = E_{HIP}(1 - CBQR)/(E_{PAH}V_bBSA(1 - Ht)FF),$$

where FF denotes the filtration fraction. As above, $E_{HIP}$, $E_{PAH}$, and CBQR are assigned the values 0.80, 0.925, and 0.24, respectively. For $V_b$, 2,405 ml per m$^2$ is used (for men and women) (*13*). The hematocrit and the filtration fraction are given their normal mean values in adults of 0.45 and 0.20, respectively (*13,15*). Insertion of these values in the expression for $|\lambda_{pk}|/SGFR$ yields 0.00144 ml$^{-1}$. The slope of the regression line for the material of 31 patients was 0.00129 ± 0.00011 ml$^{-1}$ ($\bar{x} \pm 1$ s.e.m.). The two estimates of the slopes are not significantly different ($p<0.17$). These findings strongly indicate that the rate constant $/\lambda_{pk}/$ actually reflects the ratio of the [$^{123}$I]hippuran clearance to the vascular hippuran distribution volume. Huleh et al. (*18*) found the renal plasma flow to be ~4% greater on the left side than on the right. This is comparable with the mean fractional renal clearance of [$^{123}$I]hippuran in this study,which is 3% greater on the left side than on the right (Table 2), a difference which is significant ($p<0.05$).

The literature on the distribution of the mean transit times of radioactive indicator through the whole kidney and the renal parenchyma is still very scarce. For [$^{123}$I]hippuran, we have not found any data, but two studies deal with [$^{99m}$Tc]diethylenethiaminepentaacetic acid (DTPA) transit times. Vivian et al. (*19*) investigated the transit times of [$^{99m}$Tc]DTPA in 11 children with unilateral renal diseases under two different physiological conditions: an early morning scan (EMS) and, 24 hr later, following hypotonic volume expansion (HVE). The results for the contralateral normal kidneys were: whole kidney: 400 ± 117 sec (EMS) and 161 ± 39 sec (HVE), and renal parenchyma: 140 ± 45 sec (EMS) and 120 ± 20 sec (HVE).

In our work, the MTT-values for the whole kidney and the renal parenchyma averaged 312 sec and 174 sec, respectively (Table 3) (with 60 sec being added to correct for differences in definition of zero time). Since the children in our study were moderately hydrated, it is to be expected that our mean MTT-values fall between those obtained at the HVS and the EMS studies. This is true as regards the mean MTT-value for the whole kidney, whereas our mean parenchymal transit time exceeds that obtained at the EMS. Since we are using logarithmic normal distributions for the MTT-values, the scatter of the mean transit time distributions cannot readily be compared.

Piepsz et al. (*20*) found a mean renal MTT for [$^{99m}$Tc]DTPA of 216 ± 66 sec in their study comprising more than 800 children and adults. This distribution of MTT is clearly below our values. However, Piepsz and coworkers stated than an MTT-value for the whole kidney above 8.5 min gave rise to a suspicion of obstruction or residual postoperative dilatation. In their material, this was incorrect in only 5% of the cases studied. The one-tailed upper 5% significance limit for the renal MTT in our material was 9.2 min (Table 3) (again with 1 min being added to correct for differences in zero time).

In regard to the four children with prolonged renal MTT, a failure in hydration prior to the renography can be the explanation in only one of them. Patient II had bilaterally prolonged renal MTT-values and a low estimated diuresis whereas the other three patients had unilaterally prolonged renal MTT and a normal/high estimated diuresis.

Renograms with delayed peak times and slowly decreasing curves after the peak in patients considered normal have been reported (*21*). The MCU performed on the day prior to the IHGR might have caused a new urinary tract infection. However, others (*20*) have shown that the MTTs are not affected in patients suf-

fering from such infections.

According to Whitfield et al. (*8*), prolonged renal transit times are caused by obstructive uropathy and accompanied by a dilated renal pelvis. If, in addition, the parenchymal transit times are prolonged, the obstructive uropathy has induced obstructive nephropathy. In our four patients, no dilated renal pelves were demonstrated radiologically or with ultrasonography. We believe that the findings in the four children indicate that the dilution of the urine in the distal tubuli can be subject to large variations in the same person at different times and also between the two kidneys at the same time.

We conclude that patients with MTT-values within the 5% significance limits determined in Table 3 can be considered normal as regards the passage of [$^{123}$I]hippuran through the kidneys. Patients with renal MTT-values above the 5% significance limits should not necessarily be considered having an abnormal renal function. The patient material in the study of the precision of the quantitative method represents several patients with impaired renal uptake function, decreased [$^{123}$I]hippuran clearance, and prolonged transit time of indicator. Hence, this material is believed to be suitable for investigation of the precision. The results showed a relative precision of the seven variables determined between 3 and 13%. This reproducibility is considered satisfactory.

## APPENDIX 1

The model of pre-renal indicator kinetics is shown in Fig. 5. It consists of a plasma compartment of volume $V_p$ with an indicator concentration $C_p(t)$ and an extravascular compartment of volume $V_e$ with an indicator concentration $C_e(t)$. The intercompartmental indicator clearance is denoted $F_i$.

Assuming first order kinetics of the kidneys with respect to the radioactive indicator in the plasma, the concentrations $C_p(t)$ and $C_e(t)$ in the two compartmental model are determined by a set of first order homogeneous linear differential equations with constant coefficients:

$$\frac{d}{dt}\begin{Bmatrix}C_p\\C_e\end{Bmatrix} = \begin{Bmatrix}-(F_{pk}+F_i)/V_p & F_i/V_p\\ F_i/V_e & -F_i/V_e\end{Bmatrix}\begin{Bmatrix}C_p\\C_e\end{Bmatrix}. \quad \text{(A1.1)}$$

The type of solution for this system of differential equations depends on the eigenvalues of the coefficient matrix. The two eigenvalues are denoted $\lambda_1$ and $\lambda_2$. It can be shown that $\lambda_1$ and $\lambda_2$ are distinct, negative real numbers (*1*).

With this knowledge of $\lambda_1$ and $\lambda_2$, the solution to the differential equations in Eq. (A1.1) can be expressed as sums of two exponentials in $\lambda_1$ and $\lambda_2$:

$$C_p(t) = CP_1e^{\lambda_1 t} + CP_2e^{\lambda_2 t} \quad \text{and}$$
$$C_e(t) = CE_1e^{\lambda_1 t} + CE_2e^{\lambda_2 t}.$$

The values of the coefficients ($CP_1$, $CP_2$) and ($CE_1$, $CE_2$) depend on the initial conditions, $C_p(o)$ and $C_e(o)$, whereas the rate constants $\lambda_1$ and $\lambda_2$ are independent of the initial conditions.

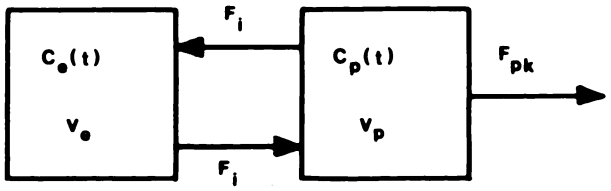


**FIGURE 5**
**Model of prerenal indicator kinetics as open two compartmental model consisting of plasma compartment of volume $V_p$ and extravascular compartment of volume $V_e$. Indicator concentrations in the two compartments are $C_p(t)$ and $C_e(t)$, respectively. $F_{pk}$ is renal plasma clearance of indicator, while $F_i$ denotes intercompartmental clearance of indicator**

## APPENDIX 2

Let $t_o$ and $t_o + \Delta t$ denote two times after injection when indicator has not yet started to leave the kidney.

Then we have:

$$K(t_o) = \rho \cdot \int_0^{t_o} H(t)dt \text{ and} \quad \text{(A2.1)}$$

$$K(t_o + \Delta t) - K(t_o) = \rho \cdot \int_{t_o}^{t_o+\Delta t} H(t)dt, \quad \text{(A2.2)}$$

where $\rho$ is a proportionality constant of dimension inverse time.

Insertion of Eq. (12) into Eqs. (A2.1-2) gives:

$$CK(t_o) - SF \cdot RBG(t_o) = \rho \cdot \int_0^{t_o} H(t)dt \quad \text{(A2.3)}$$

and

$$CK(t_o + \Delta t) - CK(t_o) - SF \cdot (RBG(t_o + \Delta t) - RBG(t_o)) = \rho \cdot \int_{t_o}^{t_o+\Delta t} H(t)dt. \quad \text{(A2.4)}$$

Division of Eq. (A2.3) by (A2.4) gives:

$$\frac{CK(t_o) - SF \cdot RBG(t_o)}{\Delta CK - SF \cdot \Delta RBG} = R,$$

which is easily solved for SF to give Eq. (13).

## APPENDIX 3

The convolution integral in Eq. (15)

$$\int_0^t RIR(T) \cdot KI(t-T)dT = K(t)$$

is transformed by means of the convolution rule in the theory of Laplace transforms:

$$L\left\{\int_0^t RIR(T) \cdot KI(t-T)dT\right\} = RIR(s)KI(s), \quad \text{(A3.1)}$$

where

$$RIR(s) = L\{RIR(t)\} \quad \text{(A3.2)}$$

and

$$KI(s) = L\{KI(t)\}. \quad \text{(A3.3)}$$

The Laplace transformation $L\{f(t)\}$ of a function $f(t)$ is defined as:

$$L\{f(t)\} \equiv f(s) = \int_o^\infty e^{-s\cdot t} f(t)dt,$$

where s is a complex number. For

$$K(s) = L\{K(t)\} \quad \text{(A3.4)}$$

we get from Eqs. (A3.1-4) that

$$RIR(s)KI(s) = K(s) \quad \text{(A3.5)}$$

and that

$$RIR(t) = L^{-1}\{K(s)/KI(s)\}, \quad \text{(A3.6)}$$

where $L^{-1}\{\ \}$ indicates the inverse Laplace transformation.

The following derivations consist of three steps: (a) the Laplace transform of the kidney curve K(t); (b) the Laplace transform of the kidney input KI(t); and (c) the inverse Laplace transform of the ratio K(s)/KI(s).

At this point, it is more convenient that zero time is $t_o$ min postinjection and not the injection time. A new time variable, denoted T, is introduced where $T = t - t_o$.

The kidney curve, K(T), will be approximated as:

$$K(T) = \sum_{i=1}^{\infty} K(T_i)U_i(T), \quad \text{(A3.7)}$$

where the function $U_i(T)$ is defined as

$$U_i(T) = \begin{cases} o \text{ for } T < T_i - \Delta T/2 \\ 1 \text{ for } T_i - \Delta T/2 \le T \le T_i + \Delta T/2 \\ o \text{ for } T > T_i + \Delta T/2, \end{cases}$$

where $T_i = T_{i-1} + \Delta T$ (i = 2,3, ...) are the sample times of K(T); $T_1 = o$.

For K(s) we get

$$K(s) = L\left\{\sum_{i=1}^{\infty} K(T_i)U_i(T)\right\}$$

$$= \sum_{i=1}^{\infty} K(T_i)L\{U_i(T)\}$$

$$= \sum_{i=1}^{\infty} K(T_i)\cdot\frac{1}{s}\cdot(e^{-T_i^*\cdot s} - e^{-T_{i+1}^*\cdot s})$$

where $T_i^*$ denotes

$$T_i^* = T_i - \Delta T/2 \ (i = 2,3, \ldots)$$

and

$$T_1^* = T_1 = o.$$

The expression for K(s) can be rearranged to read:

$$K(s) = \sum_{i=1}^{\infty} \Delta K_i \cdot \frac{1}{s}\cdot e^{-T_i^*\cdot s}, \quad \text{(A3.8)}$$

where $\Delta K_i = K(T_i) - K(T_{i-1})$ for i = 2,3, ... and $\Delta K_1 = K(o)$.

Equation (A3.8) is the final expression for the Laplace transform of the kidney curve.

Equation (19) for the kidney input with T as the time variable reads:

$$KI(T) = K(o)\cdot\delta(o) + \gamma_1\cdot e^{\lambda_1\cdot T} + \gamma_2\cdot e^{\lambda_2\cdot T}.$$

The Laplace transform of this expression is:

$$KI(s) = K(o) + \frac{\gamma_1}{s-\lambda_1} + \frac{\gamma_2}{s-\lambda_2}$$

$$= K(o)\cdot\frac{(s-a)(s-b)}{(s-\lambda_1)(s-\lambda_2)}. \quad \text{(A3.9)}$$

The parameters a and b are determined as the roots in the quadratic expressions $s^2 + L\cdot s + M$ where

$$L = (-K(o)\cdot(\lambda_1+\lambda_2) + \gamma_1 + \gamma_2)/K(o) \text{ and}$$

$$M = (K(o)\cdot\lambda_1\cdot\lambda_2 - \gamma_1\cdot\lambda_2 - \gamma_2\cdot\lambda_1)/K(o).$$

It can be shown that the discriminant of the quadratic equation is positive and, therefore, a and b are real and distinct numbers. Furthermore, a and b must be negative (*1*).

Equation (A3.9) is the final expression for the Laplace transform of the kidney input.

Equations (A3.5) and (A3.8-9) give for the Laplace transform of RIR(T):

$$RIR(s) = \frac{1}{K(o)}\cdot\sum_{i=1}^{\infty}\Delta K_i\cdot\frac{(s-\lambda_1)(s-\lambda_2)}{s(s-a)(s-b)}\cdot e^{-T_i^*\cdot s}.$$

The residual impulse response at the time $T = T_k$ (k = 1,2, ...) is given by:

$$RIR(T_K) = \frac{1}{K(o)}\cdot\sum_{i=1}^{k}\Delta K_i\cdot\varphi(T_k - T_i^*), \quad \text{(A3.10)}$$

where the function $\phi(t)$ is defined by

$$L\{\varphi(T)\} \equiv \frac{(s-\lambda_1)(s-\lambda_2)}{s(s-a)(s-b)}.$$

The exponential term in RIR(s) is included in Eq. (A3.10) in the argument of the $\varphi$-function using the delay rule in Laplace transforms.

Equation (A3.10) is the final expression for the computation of the residual impulse response. However, the $\varphi$-function remains to be determined.

The expression for $L\{\varphi(T)\}$ is decomposed in sums of partial fractions:

$$\frac{(s-\lambda_1)(s-\lambda_2)}{s(s-a)(s-b)} = \frac{C}{s-a} + \frac{D}{s-b} + \frac{E}{s} \quad \text{(A3.11)}$$

or

$$(s-\lambda_1)(s-\lambda_2) = C\cdot s\cdot(s-b) + D\cdot s\cdot(s-a) + E\cdot(s-a)(s-b).$$

Insertion of s = a, s = b, and s = c into the last expression gives for C, D, and E, respectively, that

$$C = (a-\lambda_1)(a-\lambda_2)/(a\cdot(a-b)),$$

$$D = (b-\lambda_1)(b-\lambda_2)/(b\cdot(b-a)), \text{ and}$$

$$E = \lambda_1\cdot\lambda_2/(a\cdot b).$$

The inverse Laplace transform of the right side of Eq. (A3.11) yields the final expression for the $\varphi$-function:

$$\varphi(T) = Ce^{a \cdot T} + De^{b \cdot T} + E.$$

The $\varphi(T)$ curve starts in 1 at time zero and with E ($o < E < 1$) as asymptote for $T \rightarrow \infty$(1).

## REFERENCES


1. Carlsen O: Quantitative analysis of the I-131 hippuran renogram for evaluation of kidney function, Licentiate PhD Thesis, Institute for Numerical Analysis, Technical University of Denmark, Lyngby, 1980, pp 29-33, 131-133, 139-146, 325-335
2. Britton KE, Brown NJG: *Clinical Renography*, London, Lloyd Luke, 1971
3. Mackay A, Eadie AS, Cumming AMM, et al: Assessment of total and divided renal plasma flow by $^{123}$I-hippuran renography. *Kidney Int* 19:49-57, 1981
4. Peters M, Sippel R: Methodenvergleich zur Registrierung der Ganzkörperkurve für die Berechnung der $^{131}$J-Hippuran-Clearance. *NucCompact* 11:244-248, 1980
5. Heidenreich P, Lauer O, Fendel H, et al: Determination of total and individual kidney function in children by means of 123-I-hippuran whole body clearance and scintillation camera. *Pediatr Radiol* 11:17-27, 1981
6. Devaux S: Nierenfunktionsdiagnostik in der Kinderheilkunde mit einfachen nuklearmedizinischen Untersuchungsverfahren. *Kinderärztliche Praxis* 9:412-420, 1977
7. Diffey BL, Hall FM, Corfield JR: The $^{99m}$Tc-DTPA dynamic renal scan with deconvolution analysis. *J Nucl Med* 17:352-355, 1976
8. Whitfield HN, Britton KE, Hendry WF, et al: The distinction between obstructive uropathy and nephropathy by radioisotope transit times. *Br J Urol* 50:433-436, 1978
9. Britton KE, Nimmon CC, Whitfield HN, et al: Obstructive nephropathy: successful evaluation with radionuclides. *Lancet:* 905-907, 1979
10. Marquardt DW: An algorithm for least-squares estimation of nonlinear parameters. *J SIAM* 11:431-441, 1963
11. Becker G: *Die Nierenfunktionsanalyse mit Jod-131-Hippuran*, Heidelberg, Dr. Alfred Hüthig Verlag, 1969, pp 35-37, 66-67
12. Hoel PG: *Introduction to Mathematical Statistics*, New York, John Wiley & Sons, 1962, pp 246
13. Diem K, Lentner C, eds: *Scientific tables*, Basel, Documenta Geigy, 1970, pp 192-193, 531, 555, 617
14. Therkelsen AJ: *Medicinsk statistik*. København, Akademisk Forlag, 1976, pp 69-71
15. Wesson LG: *Physiology of the Human Kidney*, New York, Grune and Stratton, 1969, pp 96-100
16. Pihl B: *Studies on the Single Injection Technique for Determination of Renal Clearance*, Lund, Studentlitteratur, 1973, pp 99
17. Magnusson G: Kidney function studies with $^{131}$I-tagged sodium ortho-iodo-hippurate. *Acta med Scand* (Suppl 378) 171:5-119, 1962
18. Huleh WH, Baldwin DS, Biggs AW, et al: Renal function of the separate kidneys of man. I. Hemodynamics and excretion of solute and water in normal subjects. *J Clin Invest* 39:389, 1960
19. Vivian G, Barratt TM, Gordon I: Variations of normal renal DTPA transit times under different physiological conditions. VI. Congress of the European Nuclear Medicine Society, Brussels, 1983 (abstr)
20. Piepsz A, Ham HR, Hall M, et al: The clinical contribution of renal transit times in the uronephrological diseases of the child and the adult: A prospective, international joint project. *J Nucl Med* 21:P40, 1980 (abstr)
21. Daschner F, Hofmann B, Marget W: Bewertung von diagnostichen Parametern chronish rezidivierender Harnwegsinfektionen bei kindern. *Mschr Kinderheilk* 125:777-782, 1977